Elastic Properties of Short Glass Fiber-Reinforced ZA-27 Alloy Metal Matrix Composites

S.C. Sharma

(Submitted 8 September 1999; in revised form 1 December 2000)

A well-consolidated composite of ZA-27 alloy reinforced with short glass fiber at volume fractions of 2, 7, 12, and 17% was prepared by liquid infiltration techniques and its elastic properties were determined by destructive testing. The results showed that the modulus of elasticity and ultimate tensile strength of the composite gradually increased with increasing volume fraction of the fiber, although the ductility decreased with an increase in volume fraction of the fibers. In addition, the data obtained from Young's modulus measurements were compared with theoretical results predicted by the shear-lag model, Nielsen-Chen model, and computational model. The experimental results were shown to be in better agreement with those of the latter two models. The ultimate tensile strength test results were also compared with theoretical results predicted by the shear-lag and Miwa models. The Miwa model agreed favorably with the experimental results.

Keywords elastic properties, SEM, short glass fiber, theoretical model, ZA-27 alloy

1. Introduction

With recent advances in processing technology, the ability to produce a wide range of metal matrix composites (MMCs) in economically feasible quantities has increased dramatically.[1] Zinc-aluminum (ZA) alloys have emerged as potential engineering materials for a variety of applications, especially in automobile sectors. However, as they tend to loose their tensile and creep resistance above 100 °C temperature, application of these alloys is currently restricted to lower temperatures. To improve their mechanical properties at elevated temperatures, since 1980, many researchers have begun to use ceramic, glass, and carbon fibers to reinforce the alloys.[2–6]

Many researchers[7–15] have studied the elastic properties of MMCs using a variety of methods, such as the shear-lag theory,[7] finite element analysis,[8,9] boundary element analysis,[10] the Nielsen-Chen model,[11] the Eshelby model,[12] the Mori-Tanka model,[13] the Halpin-Tsai model,[14] the Mean-Field model,[15] the rule of mixtures approximation, *etc.* The shear-lag, Nielsen-Chen, and Halpin-Tasi models have been popular for predicting the properties of short-fiber composites.

In an effort to provide reliable data for comparison with the theoretical models in developing short-fiber composites, the present experiments to study elastic modulus, ultimate tensile strength (UTS), and ductility of ZA-27 alloy reinforced with short E-glass fibers, at volume fractions of 2 to 17, at 5 increments, at room temperature have been conducted. The results of the experiments are used to compare the data obtained from the shear-lag, Nielsen-Chen, and other computational models for Young's modulus. The UTS results of short fiber-reinforced composites obtained by experimental analysis were compared with those of computational shear-lag and Miwa's model.

S.C. Sharma, Research and Development, Mechanical Department Engineering, R.V. College of Engineering, Banalore-560 059, Karnataka, India. Contact e-mail: rvrdscs@blr.vsnl.net.in.

2. Experimental Work

The matrix alloy used in the present investigation was ZA-27 alloy, which has E-glass short fiber reinforcement, and the chemical composition is as shown in Table 1. Fibers in roving form were bundled and cut into short fibers of uniform length by a constant-length cutter. The short glass fiber was cleaned in distilled water and dried at 90 °C.

Composites were fabricated using a liquid infiltration method (squeeze infiltration technique described by Akbulut *et al.*[11]) A fiber preform of 10 mm diameter and 80 mm length was placed in a die preheated to 350 °C and infiltrated with liquid metal. The ZA-27 alloy was superheated by about 100 °C and injected by means of a ram traveling at about 9 mm s^{-1}, with a pressure setting of 25 to 30 MPa to the mold. The specimen was obtained after cooling the mold rapidly. The specimens (70 mm long and 6 mm in diameter) were precision-machined from the cylindrical blanks with a diamond tipped cutting tool per ASTM E-817[16] standards.

The test was performed using a Shimuzu (Japan) universal testing machine (of 10 ton capacity) equipped with a pair of extensometers. The modulus measurements were carried out on the specimens in tension, using the "loading unloading method" with a crosshead velocity of 5 mm/min. The Young's modulus values were calculated from the slope of the ruler fit straight lines joining the two ends of the loading-unloading curves. Finally, the UTS was calculated for the same specimen. This test was repeated at least four times using different specimens and the mean values and corresponding standard deviation were obtained.

The choice of a sample for microscopic study is very important for analyzing composites. Optical microscopy was used to examine the general microstructure and fiber distribution in the composite produced. To increase the visibility of the embedded fibers in the matrix, the composites were etched

Table 1 Chemical composition of ZA-27 alloy and E glass

Chemical composition ZA-27 alloy—wt.%			
Al	**Cu**	**Mg**	**Zn**
25.0–28.0	2.0–2.5	0.015–0.03	Remainder

Chemical composition of E glass—wt.%				
SiC	**Al2O3**	**CaO**	**MgO**	**B4O**
54.3	15.2	17.2	0.6	8.0

deeply with a Palmerton etching reagent[17] (chromic oxide-200 g, sodium sulfate-15 g, and water-1000 mL). Scanning electron microscopy (SEM) was performed on the fractured surface to understand the failure mechanisms.

3. Results and Discussion

3.1 Modeling

Rapid advances made in hardware and software technological fields have fundamentally changed our environment. Mathematical models are designed increasingly to support decision-making processes. Composite materials can be fabricated by choosing different combinations of matrix alloy and reinforcements. For MMCs, the matrix is usually an alloy-based material and there is also an increasing number of available reinforcements, *e.g.*, fibers, particulates, whiskers, *etc*. Regarding the prediction of properties of MMCs from the properties of the individual components, numerous mathematical modeling techniques have been formulated. Each model is bound by a set of parameters and also the data are specific for successful evaluation. There is an extremely large number of different MMCs, each having different individual properties. The reinforcement can be of a variety of types, having undergone different surface treatments; their ranges of volume fraction are also varied, They may possess different geometries (such as particles, whiskers, short fiber, and long fiber). The enormous number of different MMCs (matrix and reinforcement) has led to significant problems in manufacturing and testing activities, and the manufacturing processes adopted are very expensive. In addition to quantitative analysis of the properties of the MMCs, mathematical modeling also helps to estimate the cost of essential development and can be used in the design of MMCs to meet specific requirements.

All existing tensile models are based on the same basic assumptions, such as the matrix is linearly elastic and isotropic. The fibers are identical in shape and size, but they are either isotropic or transversely isotropic. There is a perfect interfacial bonding between the matrix and the fibers; there is also a nearly perfect bonding at their interface, and no chemical reaction between them.[18]

3.2 Elastic Modulus

The reinforcement may be regarded as acting efficiently if it carries a relatively high proportion of the externally applied load. This results in higher strength, as well as greater stiffness, because the reinforcement is usually stronger, as well as stiffer, than that of a matrix. The concept of elastic load transfer is familiar for those who are working with fiber-reinforced composites.[19]

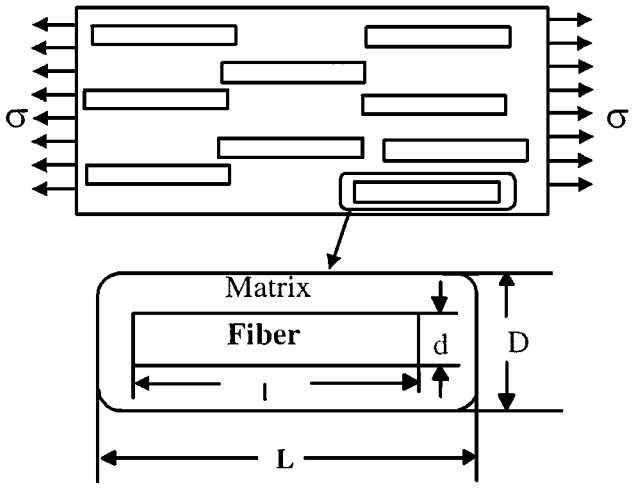

Fig. 1 Shear-lag model for aligned short fiber composite

In general, the shear-lag model equation is most appropriate to estimate the elastic properties of the aligned short fiber-reinforced composites. It is not possible to produce composite specimens with perfectly aligned fiber. Therefore, the author prefers a computational model to compare the elastic modulus of short-glass fiber-reinforced MMCs with experimental results by using computer software. The author compared computational model with the Nielsen model, which assumes approximate elastic properties of the random short fiber-reinforced MMCs.

3.3 Shear-Lag Model

Originally, the shear-lag model was developed by Cox.[20] Cox was the first to examine[21] the continuous fiber MMCs. A detailed derivation was summarized by Kelly,[22] and this model is best well suited for short fiber MMCs in which short fibers of uniform length and diameter are all aligned in the loading direction and distributed uniformly throughout the material, as shown in Fig. 1.

The elastic modulus of the composite E_c and fiber length l and detailed derivations of the shear-lag model are given in Ref 23.

$$E_c = (1 - V_f)\, E_m + V_f E_f \left\{ \frac{1 + (E_m/E_f - 1)\tanh(\beta 1/2)}{\beta 1/2} \right\} \quad \text{(Eq 1)}$$

where E_m and E_f are the Young's modulus of the matrix and the fiber, respectively. The term V_f is the volume percentage of the fibers, and β is a matrix material constant given in Ref 23.

$$\beta = 21.5/d \left[\frac{(G_m/E_f)}{\ln (D/d)} \right]^{0.5} \quad \text{(Eq 2)}$$

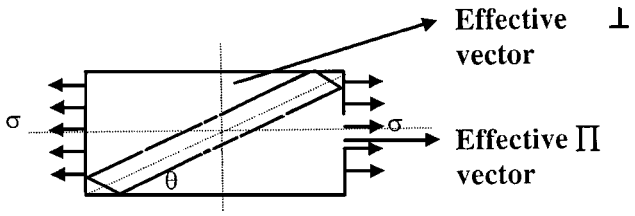

Fig. 2 Short fiber inclined at an angle (θ) to the loading direction

where G_m is the shear modulus of the matrix, with a fiber diameter d; and D is the diameter of the unit cell, which is a function of the fiber volume fraction and fiber diameter d.

Accurate experimental data are not available, since it is not possible to produce physical samples with perfectly aligned fibers. The main drawback of this model is that it estimates elastic properties only when fiber aligns to the loading direction of the composite. But, in practice, in short fiber-reinforced composites, the fibers are not aligned in the direction of the applied load. Considering this parameter, the author's computational model (Fig. 2) has been developed.

$$\theta = (\theta_1 + \theta_2 + \theta_3 + \theta_4 + \cdots + \theta_n)/n \qquad \text{(Eq 3)}$$

in which θ is the effective angle between the fiber axis and the axis of the matrix. Considering the effective angle of fiber, the Young's modulus can be resolved into two components, that is, (E_Π) Young's modulus parallel to the axis of the loading direction and ($E_\perp$) perpendicular to the axis of loading. The values of E_Π and $E_\perp$ were obtained from the rule-of-mixtures equation.

From the mixture rule (upper bound),[24]

$$E_\Pi = E_{fa}V_f + E_m(1 - V_f) \qquad \text{(Eq 4)}$$

From the mixture rule (lower bound),[25]

$$E_\perp = \frac{E_{fa}E_m}{E_{fa}(1 - V_f) + V_fE_m} \qquad \text{(Eq 5)}$$

The Young's modulus of the short fiber-reinforced composite is given by

$$E_c = \sqrt{(E_\Pi \cos\theta)2} + (E_\perp \sin\theta)^2 \qquad \text{(Eq 6)}$$

The effective angle of the fibers (θ) was computed by using the software developed by the author, which is shown in the form of a flowchart (Fig. 3). From this software, the effective fiber angle $\theta = 161.83V_f^{0.4027}$ was obtained.

3.4 Nielsen-Chen Model

Bert[25] has given another model describing the elastic properties of random fiber composites based on the approach originally introduced by Nielsen-Chen, in which

$$E_c = 3/8\ E_\Pi + 5/8\ E_\perp \qquad \text{(Eq 7)}$$

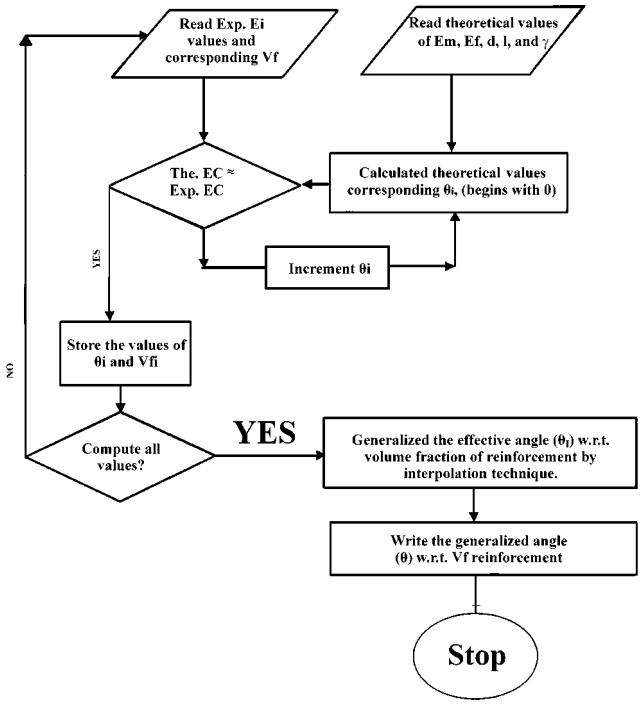

Fig. 3 Flow chart for the computation of effective fiber angle (θ)

$$E_\Pi = E_fV_f + E_m(1 - V_f) \qquad \text{(Eq 8)}$$

and

$$E_\perp = \frac{E_fE_m}{E_f(1 - V_f) + V_fE_m} \qquad \text{(Eq 9)}$$

Another equation proposed by Nielsen-Chen takes into account the Poisson's ratio and gives a better fit to the experimental results, *viz.*

$$E_\perp = \frac{E_fE'_m}{E_f(1 - V_f) + V_fE'_m} \qquad \text{(Eq 10)}$$

where

$$E'_m = E_m/(1 - \gamma_m^2) \qquad \text{(Eq 11)}$$

3.5 Strength

Nardone and Prewo[26] have proposed a computational shear-lag theory to describe the strengthening of the composites. They have postulated that the redistribution of the matrix stress to the reinforcement through interfacial shear load transfer is the main contributing factor resulting in the significant increase in yield strength.

The theoretical UTS of the composite is expressed as (computational shear-lag model)[27]

$$\sigma_c/\sigma_m = 0.5\ V_f(2 + 1/d) + (1 - V_f) \qquad \text{(Eq 12)}$$

where σ_{yc} and σ_{ym} are, respectively, the yield stresses of the composite and the matrix.

In the Miwa model,[28,29] the tensile strength σ_c of a composite, in which the short fibers are arranged in a random planar orientation, depends strongly on the yield shear strength at the fiber-matrix interface and is written as

$$\sigma_c = \frac{2\tau}{\pi}\left(2 + \ln\left(\frac{\tau(L/d)\sigma_m V_f + \sigma_m^2 V_m}{\tau^2}\right)\right) - \sigma_r \qquad \text{(Eq 13)}$$

where L is the fiber length; d is the fiber diameter; and σ_f and σ_m are the tensile strengths of the fiber and matrix, respectively. The terms V_f and V_m are the volume of the fiber and matrix, respectively. The term σ_r is the thermal stress produced during molding of the composite by the difference in the thermal expansion coefficient between the fiber and matrix material and is given by the following equation:

$$\sigma_r = \frac{2(\alpha_m - \alpha_f)E_m \Delta T}{(1 + \gamma_m) + (1 + \gamma_f)(E_m/E_f)} \qquad \text{(Eq 14)}$$

where α is the coefficient thermal expansion, E is the Young's modulus, γ is the Poisson's ratio, and ΔT is the difference temperature from the melting temperature of the matrix alloy to the room temperature. The suffixes m and f are the matrix and reinforcement fiber, respectively.

3.6 Experimental Results

Tensile Properties. At the room temperature, only a low to moderate increase in strength is observed in short fiber-reinforced composites as the fibers are not oriented unidirectionally.[30] The tensile properties of the ZA-27/short glass fiber composite at laboratory temperature are summarized in graphs (the results reported are the mean values). The standard deviations were obtained from four experiment trials.

Elastic Modulus. The measured mean values of elastic moduli were plotted as a function of volume percentage of short glass fiber reinforcement, as shown in the Fig. 4. McDanels[31] is of the opinion that the elastic modulus increases with an increase in reinforcement content. However, the elastic modulus has been found to be independent of the type of reinforcement. As the short glass fiber content was increased from 1 to 17% by volume, an improvement in Young's modulus of 13.26% has been observed. The sharp increase in Young's modulus has been observed by the author, and is probably due to the homogenous distribution of fibers and the alignment of these fibers parallel to the axis with minimum segregation in the composite.

The Young's modulus of the composite increased at lower rates when the volume fraction of the reinforcement of the composite is in the range of 7 to 17. This may be attributed to the changes in the effective angle of alignment of fiber with respect to the loading direction.

Comparison of the Experimental Results with the Theoretical Calculation. In this part, the experimental results were compared with the theoretical data obtained from the shear-lag, computational and the Nielsen-Chen models. Figure 4 shows plots of the Young's modulus comparing the experimental data with the theoretical data obtained from the shear-lag and Nielsen-Chen models for the reinforced composites with 2, 7, 12, and 17 short glass fibers in volume fraction, respectively. The Nielsen-Chen model is in better agreement with the experimental value when compared with the shear-lag model; the shear-lag model is well suited at lower volume fractions, but at higher volume fractions, it overestimates the Young's modulus. The shear-lag model assumes that fibers are aligned in the loading direction. Such alignment of short fibers in composites is not possible to produce by present casting techniques. Therefore, the author has considered the effective angle of the aligned fiber in the composite adopting the shear-lag model to develop the computational model using the computer software in C++, which compares with the experimental data shown.

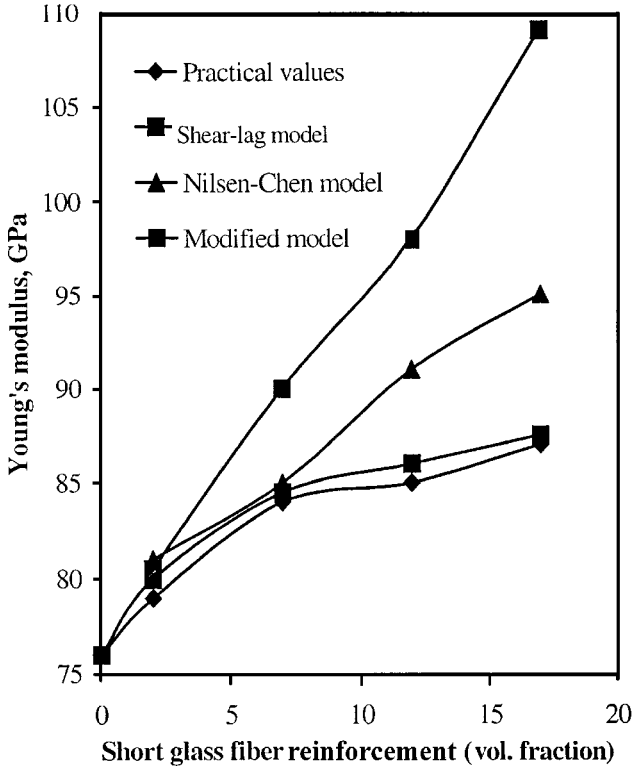

Fig. 4 Comparison of the experimental and theoretical values of Young's modules for ZA-27/short glass fiber composites

Tensile Properties. Figure 5 shows the effect of short glass fiber on the UTS in ZA-27 alloy composites. It can be seen that, as the fiber content is increased, the UTS of the composite material is also increased. There is a marked increase in the UTS of the composite from 15.5 to 28.7% as the short glass fiber content is increased from 2 to 17 volume fraction. The increase in UTS is attributed to the presence of hard glass fibers, which impart strength to the matrix alloy, thereby providing enhanced tensile strength. Vogelsang *et al.*[32] believes that the improvement in UTS may be due to the matrix strengthening. The reasons assigned are the reduction in the composite grain size and the generation of a high dislocation density in the matrix, which is a result of the difference in thermal expansion between the metal matrix and the glass fiber reinforcement.

Comparison of the Experimental Results with the Theoretical calculation. The experimental results were compared

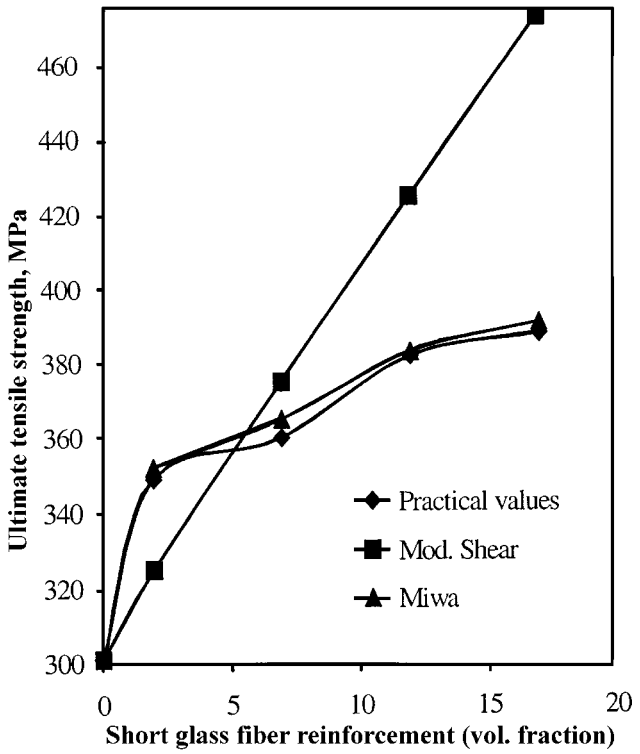

Fig. 5 Comparison of the experimental and theoretical UTS values

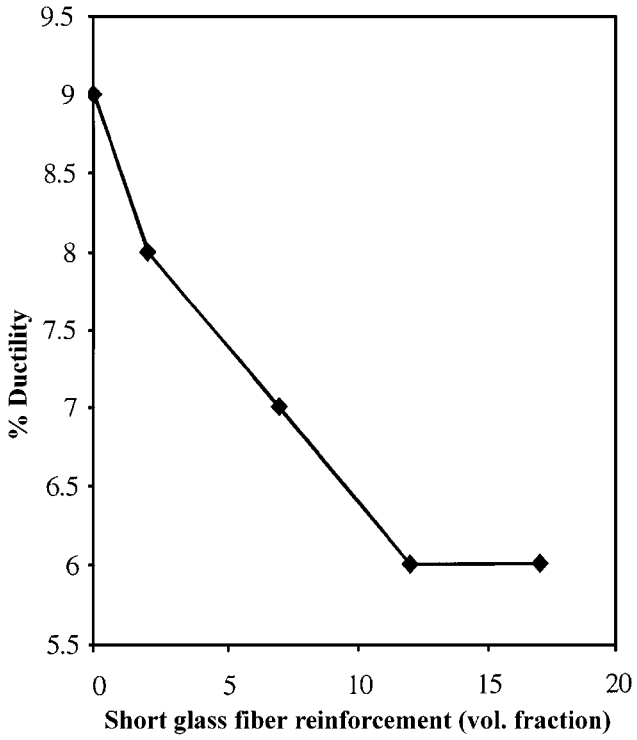

Fig. 6 Experimental values of percent ductility for the ZA-27/glass composites

with the theoretical data obtained from the computational shear-lag model and Miwa's model. Figure 5 shows the comparison between the experimental data and the theoretical data. All experimental values of the composite are in better agreement with the values predicated by the Miwa's model than with the computational shear-lag model. In the shear-lag model, it has been assumed that the fiber was aligned in the loading direction, but all fibers were not aligned in the loading direction. Miwa has developed a model for random fiber distribution with differences in the coefficient of thermal expansion of the matrix material and reinforcements, and it is believed that the tensile strength depends strongly on the yield shear strength at the fiber-matrix interface.

Ductility. Figure 6 shows the effect of the glass fiber content on the ductility (percent of elongation) of the composite. It can be seen from the graph that the ductility of the composite decreases with the increase in glass content from 2 to 17 volume fraction (the ductility decrease by about 35.9%). This decrease in ductility in the composite is the commonly encountered disadvantage in discontinuous reinforcement MMCs[33] when compared with the base alloys. Mummery *et al.*[34] is of the opinion that this behaviour is probably due to the voids, which nucleate during the plastic strains of the reinforcement or by reinforcement interface.

Optical and Scanning Electron Microstructure Analysis. The general features of the microstructure, *e.g.*, fiber distrbution, volume fraction, and orientation, were studied using an optical microscope and fractured surfaces were studied using a scanning electron microscope.

Optical micrographs in Fig. 7 show the microstructure of the composite containing 17 volume fraction of short glass

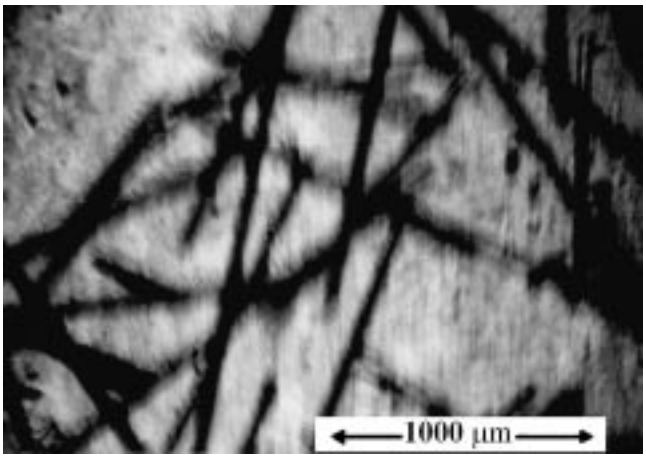

Fig. 7 Optical micrograph showing the uniform distribution of the short glass fibers in the alloy matrix (17 volume fraction)

fibers. On the macroscale, the glass short fibers used are distributed within the matrix. Figure 7 shows the planar and transverse sections of the 12% fiber-reinforced composite.

Typical fractured surfaces of ZA/glass fiber composite, obtained from tensile tests, are shown Fig. 8(a). According to Withers,[36] the experimental observation also suggests that short fibers rarely fracture. Only very few fibers can be seen as fractured and there is also evidence of ductile failure in the matrix. The failure is that few fibers split longitudinally and transversally, as shown in Fig. 8(b). The failure of fibers in the composite may be attributed to the increase in stress on the

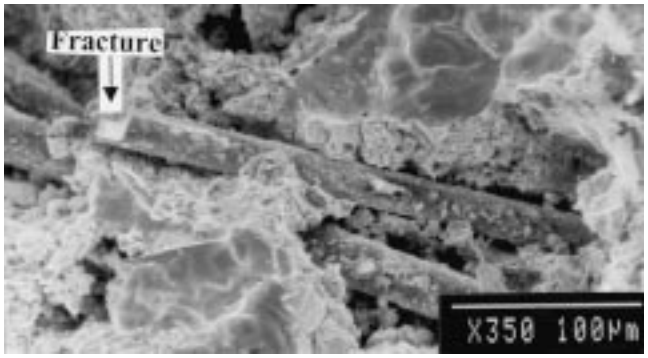

(**a**)

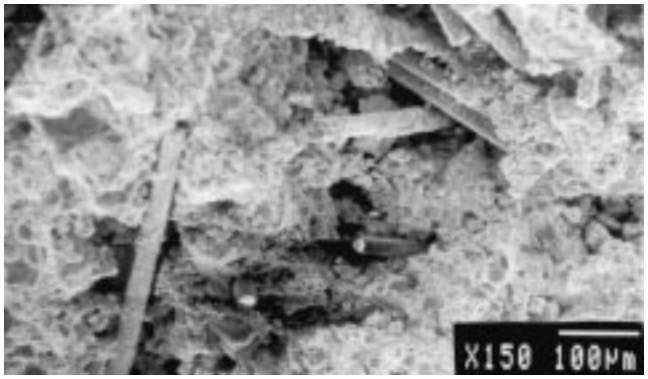

(**b**)

Fig. 8 Fractrographs of the tensile specimen shows (**a**) fractured short glass fibers and (**b**) fiber pullout from the specimen

specimen. As the load on the fiber increases, it induces strain in the fibers, and the most heavily loaded fiber fractures.[36] Some fiber "pullout" occurs in the samples, but the failure appears to be at the matrix end and not at the interfacial regions, as indicated by the conical cavities with rippled surface. Apparently, more pullout occurred in the matrix composite as expected due to the lower strength of the matrix. In some places where the fiber end was exposed to SEM, it appears that the matrix sheared away from the fiber.[37]

The SEM examination of the fractured surfaces revealed a dimpled fracture surface for the unreinforced material. The fracture surface of the unreinforced material contained a rather uneven distribution of large dimples connected by sheets of smaller dimples, indicating a pattern resulting from ductile void growth coalescence and failure (Fig. 9). The fractured surface of the reinforced material contained only smaller dimples (Fig. 8a and b) than the fractured surface of the unreinforced material.

4. Conclusions

- Homogeneous dispersions of short glass fibers could be obtained by adopting liquid infiltration techniques.
- The Nielsen-Chen model, computational model, and Miwa model can provide effective tools for the parametric studies of elastic properties of short fiber-reinforced composite materials.

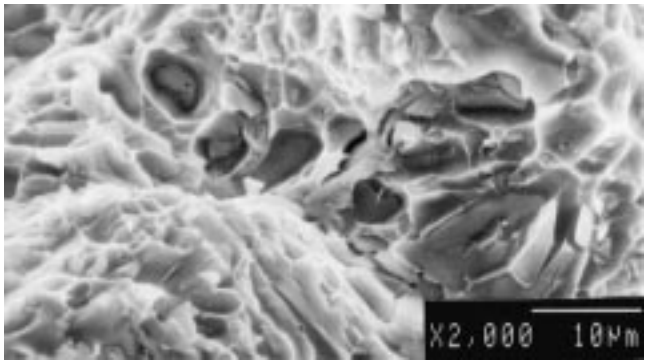

Fig. 9 Fractographs of the tensile specimen (unreinforced) show uneven distribution of the large dimples

- Comparison with experimental results shows that the theoretical models can be used to predict the elastic properties of the composite material.
- The Young's modulus and UTS of the composite material increase with an increase in the fiber volume fraction.
- The ductility of the MMC decreases gradually with an increase in the fiber volume fraction.

References

1. T. Christman, A. Needleman, S. Nutt, and S. Suresh: *Mater. Sci. Eng.*, 1989, vol. A (107), p. 49.
2. A.A. Das, B. Zantout, M.M. Yakoub, and A.J. Clegg: Proceedings of a Conference on Interfaces in Metal Matrix Composites, TMS-CIM, Montreal, 1986, p. 213.
3. R. Guerriero, J.B. Parse, and I. Tangerine: *Proc. Int. Symp.*, TMS-CIM, Montreal, 1986, p. 229.
4. Sirong Yu, Zhenming He, and Kai Chen: *Wear*, 1996, vol. 198, p. 108.
5. D.L. Gilmore, H.N. Han, and S. Derby: *Mater. Sci. Technol.*, 1998, vol. 14, p. 933.
6. Y. Kagawa and E. Nakata: *J. Mech. Sci. Lett.*, 1992, vol. 11, p. 176.
7. V.C. Nardone and K.M. Prewo: *Scripta Metall.*, 1986, vol. 20, p. 43.
8. H. Huang and M.B. Bush: *Mater. Sci. Eng.*, 1997, vol. A232, p. 63.
9. H. Toda, T. Gouda, and Kobayashi: *Mater. Sci. Technol.*, 1998, vol. 14, p. 925.
10. M.B. Bush: *Mater. Sci. Eng.*, 1992, vol. A154, p. 139.
11. H. Akbulut, M. Durman, and F. Yilmaz: *Mater. Sci. Technol.*, 1998, vol. 14, p. 299.
12. J.D. Eshelby: *Proc. R. Soc. A*, 1957, vol. 241, p. 376.
13. T. Mori and K. Tanaka: *Acta Metall.*, 1973, vol. 21, p. 571.
14. J.C. Halpin and J.L.A. Kardos: *Rev. Ploym. Eng. Sci.*, 1988, vol. 16, p. 344.
15. O.B. Pederson: *Acta Metall.*, 1983, vol. 31, p. 139.
16. ASTM Standard E8: Vol. 3.01, ASTM, Philadelphia, PA, 1993.
17. Sindney H Avner: *Introduction to Physical Metallurgy*, Tata McGraw-Hill, New York, NY, p. 22.
18. L. Charles, III Tucker, and Erwin Liang: *Comp. Sci. Technol.*, 1999, vol. 59, p. 655.
19. T.W. Clyne and P.J. Withers: *An Introduction to Metal Matrix Composites*, University of Cambridge, Cambridge, United Kingdom, 1993, p. 9.
20. H.L. Cox: *Br. J. Appl. Phys.*, 1952, vol. 3, p. 72.
21. B.W. Rosen: *AIAA J.*, 1964, vol. 2, p. 91.
22. A. Kelly: *Strong Solids*, 2nd ed., Applied Science Publisher Ltd., London, 1973, ch. 5.
23. V.C. Nardone and K.M. Prewo: *Scripta Metall.*, 1986, vol. 20, p. 43.

24. W.D. Kingery, H.K. Bown, and R.H. UHL Mann: Introduction of Metal Matrix Composites, 2nd ed., Wiley, New York, NY, 1975, p. 773.
25. C.W. Bert: *Proc. 34th SRI/RP Conf. Composite Materials Mechanics*, New York, NY, Sept. 1979, Society of Plastic Industry, University of Delaware, paper no. 20A.
26. V.C. Nardone and K.M. Prewo: *Scripta. Matall.* 1986, vol. 20, p. 43.
27. M. Taya and R.J. Arsenault: *Scripta Metall.*, 1993, vol. 41, p. 349.
28. M. Miwa, A. Nakayama, T. Ohsawa, and A. Hasegawa: *J. Appl. Polym. Sci.*, 1979, vol. 23, p. 2957.
29. M. Miwa, T. Ohsawa, and K. Tahara: *J. Appl. Polym. Sci.*, 1980, vol. 25, p. 795.
30. S. Bengtsson and R. Warren: *Mater. Sci. Technol.*, 1993, vol. 9, p. 319.
31. D.L. McDanels: *Meallt. Trans. A*, 1985, vol. 16A, p. 1105.
32. M. Vogelsang, R.J. Arsenault, and R.M. Fisher: *Metall. Trans. A*, 1986, vol. 17A, p. 379.
33. W. Beitz and K.H. Kuttner: *Dubbel Handbook of Mechanical Engineering*, Springer-Verlag, London, 1994, p. 8.
34. P.M. Mummery, B. Derby, and C.B. Scruby: *Acta Metall.*, 1993, vol. 41, p. 1431.
35. N.J. Musson and T.M. Yue: *Mater. Sci. Eng.*, 1991, vol. 135A, p. 237.
36. P.J. Withers, W.M. Stobbs, and A.J. Bourdillon: *J. Microsc.*, 1998, vol. 151, p. 159.
37. C.G. Levi, G.J. Abbaschian, and R. Mehrabian: *Metall. Trans. A*, 1978, vol. 9A, p. 697.